

A NEW POLARIZED ATMOSPHERIC RADIATIVE TRANSFER MODEL

K. F. EVANS and G. L. STEPHENS

Atmospheric Science Department, Colorado State University, Fort Collins, CO 80523, U.S.A.

(Received 22 March 1991)

Abstract—A plane-parallel polarized radiative transfer model is described. The model is used to compute the radiance exiting a vertically inhomogeneous atmosphere containing randomly-oriented particles. Both solar and thermal sources of radiation are considered. A direct method of incorporating the polarized scattering information is combined with the doubling and adding method to produce a relatively simple formulation. Several numerical results are presented for verification and comparison.

1. INTRODUCTION

This paper deals with a numerical model that solves the polarized radiative transfer equation for a plane-parallel, vertically-inhomogeneous scattering atmosphere. The full polarization characteristics of randomly-oriented particles with any shape having a plane of symmetry are taken into account. Both thermal sources and a collimated (solar) source of radiation are included in the formulation. The angular field of the radiation is represented with a Fourier series in azimuth angle and discretization of zenith angle. The model calculates the monochromatic polarized radiation emerging from an atmosphere and is hence best suited for use in remote sensing applications.

The solution method for the multiple-scattering aspect of the problem is that of doubling and adding. This approach computes the radiative properties of the medium rather than the radiance field itself so that radiances exiting the atmosphere may be easily found for many boundary conditions after the solution is computed. Doubling and adding is numerically stable for large optical depths and has the distinct advantage of conceptual simplicity. The necessity to rotate the polarization reference plane in the transformation from the single-scattering phase function to the radiative-transfer scattering matrix is the major complication of polarized models over scalar models. A simple direct method, heretofore inadequately described in the literature, is used for the transformation. The model described here is available for distribution in a well documented FORTRAN implementation. The model formulation and algorithm are described in Secs. 2-4, and example results verifying the model are presented in Secs. 5-7.

2. DESCRIPTION OF SOLUTION METHOD

An outline of the solution method is as follows. The polarization and angular aspects of the radiance field are expressed by a vector in a radiance basis. The scattering source integral in the radiative-transfer equation is correspondingly represented by matrix multiplication. The matrix differential equation is then effectively integrated with the doubling and adding method starting from infinitesimal layers. Since this formulation applies to the radiative properties of the medium (see the interaction principle below) rather than the radiation field itself, the boundary conditions are naturally dealt with after and separately from the integration.

The monochromatic plane-parallel polarized radiative transfer equation for randomly-oriented particles is

$$\mu \frac{d\mathbf{I}(\tau, \mu, \phi)}{d\tau} = -\mathbf{I}(\tau, \mu, \phi) + \frac{\hat{\omega}}{4\pi} \int_0^{2\pi} \int_{-1}^1 \mathbb{M}(\mu, \phi; \mu', \phi') \mathbf{I}(\tau, \mu', \phi') d\mu' d\phi' + \sigma(\tau, \mu, \phi), \quad (1)$$

where \mathbf{I} is the diffuse radiance field expressed as a four-vector of Stokes parameters (I, Q, U, V), \mathbb{M} is the four-by-four scattering (or Mueller) matrix, σ the Stokes vector of radiation sources, $\tilde{\omega}$ the single-scatter albedo, τ the optical depth, μ the cosine of the zenith angle, and ϕ the azimuth angle. The coordinate system used here is that τ increases downward and μ is positive for downward directions. The sources of diffuse radiation are unpolarized thermal emission and a "pseudo-source" of single scattered solar radiation:

$$\sigma(\mu, \phi) = (1 - \tilde{\omega})B(T) \begin{pmatrix} 1 \\ 0 \\ 0 \\ 0 \end{pmatrix} + \frac{F_0 \tilde{\omega}}{\mu_0 4\pi} \exp(-\tau/\mu_0) \mathbb{M}(\mu, \phi; \mu_0, \phi_0) \begin{pmatrix} 1 \\ 0 \\ 0 \\ 0 \end{pmatrix}, \quad (2)$$

where $B(T)$ is the Planck blackbody function, F_0 the unpolarized solar flux at the top of the atmosphere, and (μ_0, ϕ_0) the direction of the collimated solar beam.

The angular variation of radiation is expressed as a Fourier series in azimuth and by discretization in zenith angle using numerical quadrature. The model has several types of numerical quadrature available, including Gaussian, Lobatto, and double-Gaussian schemes. The radiance at a particular optical depth is thus represented by a vector in a radiance basis involving three components: Stokes parameters, quadrature zenith angles, and Fourier azimuth modes. The radiance field is separated according to hemisphere, with I^+ representing downward radiance ($\mu > 0$) and I^- representing upward radiance ($\mu < 0$). The number of Stokes parameters used may be less than four (reducing the vector length and speeding the computations) depending on the particular problem being solved. The number of quadrature angles and azimuth modes is governed by the desired accuracy of the radiance field. If only thermal sources are considered, then the problem is azimuthally symmetric so that only I and Q Stokes parameters and just one Fourier mode need be considered.

The key concept behind the doubling and adding method is the interaction principle, which expresses the linear interaction of radiation with a medium. The radiation emerging from a layer is related to the radiation incident upon the layer together with the radiation generated within the layer (Fig. 1). With the formulation in terms of a radiance vector, the interaction principle is

$$\begin{aligned} I^- &= T^+ I_0^+ + R^+ I^- + S^+, \\ I_0^- &= T^- I^- + R^- I_0^- + S^-, \end{aligned} \quad (3)$$

where T is the transmission matrix, R the reflection matrix, and S the source vector.

When the layer in question is the whole atmosphere (together with the surface), computing R , T , and S amounts to solving the radiative transfer equation. On the other hand, relating R , T , and S for an infinitesimal layer to the single-scattering properties is simple. Thus, there are two parts to the solution method: first, converting the single-scattering information into a form suitable for applying the interaction principle and, second, using the doubling and adding method to compute the properties of the whole atmosphere from the local (infinitesimal layer) properties.

3. TRANSFORMATION OF SINGLE SCATTERING INFORMATION

The transformation of single-scattering information from a convenient input format (say a Legendre series in the scattering angle) to a form suitable for the radiative-transfer model is complicated by the dependence of the Q and U Stokes parameters on a reference plane. For single-scattering computations, the natural reference frame is the scattering plane while for a

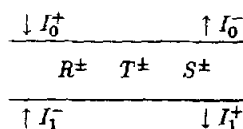


Fig. 1. A schematic illustration of the interaction principle. The I_0^+ and I_0^- on the left represent the incident radiation, and the I^- and I^+ on the right represent the emergent radiation. The R , T , and S are the reflection, transmission, and source terms, respectively, which describe how the medium interacts with the radiation.

radiative transfer calculation, the convenient reference frame is the meridional plane (defined by the z -axis and the direction of travel). The polarization transformation from the phase matrix \mathbb{P} to the scattering matrix \mathbb{M} is expressed mathematically by¹

$$\mathbb{M}(\theta, \phi; \theta', \phi') = \mathbb{L}(i_2 - \pi)\mathbb{P}(\cos \Theta)\mathbb{L}(i_1). \tag{4}$$

For the (I, Q, U, V) Stokes basis, the polarization rotation matrix is

$$\mathbb{L}(i) = \begin{pmatrix} 1 & 0 & 0 & 0 \\ 0 & \cos 2i & -\sin 2i & 0 \\ 0 & \sin 2i & \cos 2i & 0 \\ 0 & 0 & 0 & 1 \end{pmatrix}, \tag{5}$$

where the rotation angle i_1 is the angle between scattering plane and the meridional plane containing the incoming ray (θ', ϕ') , and i_2 is the angle between the scattering plane and the meridional plane containing the outgoing ray (θ, ϕ) . The scattering angle Θ and the rotation angles i_1 and i_2 may be found from spherical trigonometry.

For randomly-oriented particles with a plane of symmetry the 16 element phase matrix has only the following six unique elements:²

$$\mathbb{P}(\cos \Theta) = \begin{pmatrix} P_1 & P_2 & 0 & 0 \\ P_2 & P_5 & 0 & 0 \\ 0 & 0 & P_3 & P_4 \\ 0 & 0 & -P_4 & P_6 \end{pmatrix}. \tag{6}$$

The phase matrix for spheres has $P_5 = P_1$ and $P_6 = P_3$.

Performing the polarization rotations to find the explicit form for the scattering matrix gives

$$\mathbb{M}(\theta, \theta', \phi' - \phi) = \begin{pmatrix} P_1 & P_2 \cos 2i_1 & -P_2 \sin 2i_1 & 0 \\ P_2 \cos 2i_2 & P_5 \cos 2i_1 \cos 2i_2 & -P_5 \sin 2i_1 \cos 2i_2 & -P_4 \sin 2i_2 \\ P_2 \sin 2i_2 & P_5 \cos 2i_1 \sin 2i_2 & -P_5 \sin 2i_1 \sin 2i_2 & P_4 \cos 2i_2 \\ 0 & -P_4 \sin 2i_1 & -P_4 \cos 2i_1 & P_6 \end{pmatrix}. \tag{7}$$

The elements of the phase matrix P_i are input to the radiative transfer model as Legendre series in $\cos \Theta$, namely,

$$P_i(\cos \Theta) = \sum_{l=0}^{N_l} \chi_l^{(i)} \mathcal{P}_l(\cos \Theta). \tag{8}$$

For the radiance basis we are using, the scattering matrix \mathbb{M} should be given in terms of the Fourier series in ϕ and ϕ' and at discrete quadrature angles μ_j and μ'_j , i.e.

$$\mathbb{M}(\mu_j, \mu'_j, \phi, \phi') = \sum_{m=0}^M \sum_{m'=0}^M [\mathbb{M}_{mm'}^{\text{cc}} \cos m\phi \cos m'\phi' + \mathbb{M}_{mm'}^{\text{cs}} \cos m\phi \sin m'\phi' + \mathbb{M}_{mm'}^{\text{sc}} \sin m\phi \cos m'\phi' + \mathbb{M}_{mm'}^{\text{ss}} \sin m\phi \sin m'\phi']. \tag{9}$$

Thus, a method is needed to convert from the $\chi_l^{(i)}$ representation to the $\mathbb{M}_{mm'}$ representation of the single-scattering information. In the scalar (unpolarized) radiative-transfer case, this conversion is accomplished by using the addition theorem of associated Legendre functions. The rotation of the reference frame of the polarization precludes the use of that method for finding the Fourier modes of the scattering matrix. Dave³ invented a complicated series method to calculate the modes of the scattering matrix. A simpler method was used in this model. The method used here is to perform the polarization rotation explicitly in azimuth space and then Fourier transform the results to get the scattering matrix for each Fourier azimuth mode. This method is similar to that of Ishimaru et al,⁴ except that the rotation is performed on the Stokes parameters rather than the scattering amplitudes. Hansen⁵ used a similar technique but in a much different formulation of the doubling method.

The method proceeds as follows. For each pair of quadrature angles $(\mu_j, \mu_{j'})$ and for a number of azimuth angle differences $\Delta\phi_k = \phi' - \phi$, the scattering angle Θ is found, and the Legendre series are summed for the unique elements of the phase matrix. In the most general case six series must be summed, but depending on the number of Stokes parameters used and the type of scattering (Rayleigh, Mie, etc.) less series may be needed. Equation (7) is used to compute the scattering matrix \mathbb{M} for each of the evenly spaced $\Delta\phi_k$. The number of $\Delta\phi_k$ is chosen so the highest frequency, which depends on the number of terms in the Legendre series, is completely sampled. For each pair of quadrature angles, \mathbb{M} is Fourier-transformed with an FFT to find the coefficients \mathbb{M}_m^c and \mathbb{M}_m^s for the Fourier series in $\phi' - \phi$, viz.

$$\mathbb{M}_m^c + i\mathbb{M}_m^s = \frac{(2 - \delta_{m0})}{N} \sum_{k=0}^{N-1} e^{2\pi i/N km} \mathbb{M}(\mu_j, \mu_{j'}, \Delta\phi_k). \quad (10)$$

Since the scattering matrix only depends on the difference in azimuth between the incoming and outgoing angles, the Fourier modes separate (\mathbb{M} depends only on m , rather than m and m') and

$$\mathbb{M}_{mm'}^{cc} = \mathbb{M}_{mm'}^{ss} = \mathbb{M}_m^c \delta_{mm'}, \quad \mathbb{M}_{mm'}^{cs} = -\mathbb{M}_{mm'}^{sc} = \mathbb{M}_m^s \delta_{mm'}. \quad (11)$$

The sine and cosine modes do mix, however, for a particular m . The decoupling of azimuth modes allows the modes to be solved separately, i.e., doubling and adding are performed separately for each mode. The computationally efficient FFT, however, produces all of the Fourier modes at once, so the scattering matrices for all of the modes are computed and stored before doubling and adding begins.

The explicit form of the scattering matrix given in Eq. (7) shows its special symmetries that we use. One symmetry is that negating μ and μ' simply results in negating the off-diagonal two-by-two blocks of the matrix. This symmetry means that the scattering matrix can be computed using only half the number of angles (say with $\mu > 0$). The upper left and lower right two-by-two blocks of \mathbb{M} are even functions in $\Delta\phi$, while the upper right and lower left blocks are odd functions. This symmetry allows trivial calculation of the scattering matrix for $\pi < \Delta\phi \leq 2\pi$ from the values of $0 < \Delta\phi \leq \pi$. The symmetry also means that the cosine matrices have off-diagonal blocks of zeros, and the sine matrices have diagonal blocks of zeros. Using the symmetry and also limiting the unpolarized sources of radiation to be even (by taking the solar azimuth to be zero), the scattering matrix can be reduced to a single four-by-four matrix for each azimuth mode and quadrature angle pair.

This approach requires a rearranged radiance basis using the cosine azimuth modes of the I and Q Stokes parameters and the sine modes of the U and V parameters $\hat{\mathbf{I}} = (I^c, Q^c, U^s, V^s)$. In this basis, the scattering matrix is expressed in terms of the Fourier components from the FFTs by

$$\mathbb{M}_m(\mu_j, \mu_{j'}) = \begin{pmatrix} M_{11}^c & M_{12}^c & M_{13}^s & M_{14}^s \\ M_{21}^c & M_{22}^c & M_{23}^s & M_{24}^s \\ -M_{31}^s & -M_{32}^s & M_{33}^c & M_{34}^c \\ -M_{41}^s & -M_{42}^s & M_{43}^c & M_{44}^c \end{pmatrix}. \quad (12)$$

This form of the scattering matrix is used to find the infinitesimal layer reflection and transmission matrices as well as the pseudo-source vector of single scattered sunlight.

It is important to have the discretized scattering integral exactly integrate the phase matrix so that energy will be conserved. This means that for a given number of quadrature zenith angles there is a limit on the number of terms in the Legendre series representing the phase matrix. The model truncates the Legendre series differently according to the type of quadrature, e.g., for Gaussian quadrature, $L_{\max} = 4N_\mu - 5$ where N_μ is the number of quadrature angles per hemisphere. Achieving phase function normalization by the use of this method can be difficult for highly-peaked phase functions (scattering from large size parameter particles) because of the large number of quadrature angles required. Other techniques such as the Delta- M method⁶ are more appropriate in those circumstances.

4. APPLICATION OF DOUBLING AND ADDING METHOD

The doubling and adding sequence of operations are performed as matrix and vector operations in a radiance basis. With the above background the form of the radiance vectors can now be made explicit. Since the Fourier azimuth modes are treated separately the radiance basis consists of the Stokes parameters at the quadrature zenith angles in a hemisphere. The structure of the radiance vectors is

$$\bar{I} = \begin{pmatrix} \hat{I}(\mu_1) \\ \hat{I}(\mu_2) \\ \vdots \\ \hat{I}(\mu_N) \end{pmatrix}, \quad \hat{I}(\mu_j) = \begin{pmatrix} I^c \\ Q^c \\ U^s \\ V^s \end{pmatrix}, \quad (13)$$

where the μ_j are the quadrature points of the cosine of zenith angle and the c and s subscripts refer to the cosine and sine azimuth modes. The length of the radiance vector is thus $N_{\text{Stokes}} \times N_\mu$.

The scattering matrix defined above may now be related to the local reflection and transmission matrices for an infinitesimal layer. In the parlance of doubling-adding this step is called initialization. The model described here uses the simplest method which is sometimes called infinitesimal generator initialization. The elements of the reflection and transmission matrices and the source vector for the m th azimuth mode are

$$\begin{aligned} |T^\pm|_{ij'j'} &= \left[\delta_{ii'} \delta_{j'j'} - \frac{\Delta\tau}{\mu_j} \left(\delta_{ii'} \delta_{j'j'} - \tilde{\omega} \frac{1 + \delta_{0m}}{4} w_{j'} |\mathbb{M}_m(\pm\mu_j, \pm\mu_{j'})|_{ii'} \right) \right], \\ |R^\pm|_{ij'j'} &= \frac{\Delta\tau}{\mu_j} \tilde{\omega} \frac{1 + \delta_{0m}}{4} w_{j'} |\mathbb{M}_m(\pm\mu_j, \mp\mu_{j'})|_{ii'}, \\ |S^\pm|_{ij} &= \frac{\Delta\tau}{\mu_j} |\sigma_m(\pm\mu_j)|_i, \end{aligned} \quad (14)$$

where i is the Stokes parameter index and j is the quadrature angle index. The primed indices are the ones summed when carrying out matrix multiplication. The w_j s are the integration weights corresponding to the quadrature angles μ_j . The initial layer optical depth $\Delta\tau$ is chosen according to the desired accuracy (e.g., $\Delta\tau = 10^{-5}$ will give about five digits accuracy when using double precision). $\sigma_m(\mu_j)$ is the source term of the radiative transfer equation evaluated at the μ_j quadrature angle for the m th Fourier azimuth mode. The thermal radiation source term is isotropic so only the $m = 0$ azimuth mode contributes. The solar pseudo-source term is found by computing the scattering matrix [Eq. (12)] for the incident solar direction and outgoing quadrature angles and then multiplying by the solar flux factor as indicated by Eq. (2).

Writing down the interaction principle [Eq. (3)] for two adjacent layers and eliminating the radiances at the common interface leads to the algorithm for combining two layers. The *adding* formula computes the properties of the combined layer (T) in terms of the properties of the top layer (1) and the bottom layer (2), i.e.,

$$\begin{aligned} R_{\bar{2}}^+ &= R_2^+ + T_2^+ \Gamma^+ R_1^+ T_2^-, & R_{\bar{2}}^- &= R_1^- + T_1^- \Gamma^- R_2^- T_1^+, \\ T_{\bar{2}}^+ &= T_2^+ \Gamma^+ T_1^+, & T_{\bar{2}}^- &= T_1^- \Gamma^- T_2^-, \\ S_{\bar{2}}^+ &= S_2^+ + T_2^+ \Gamma^+ (S_1^+ + R_1^+ S_2^-), & S_{\bar{2}}^- &= S_1^- + T_1^- \Gamma^- (S_2^- + R_2^- S_1^+), \\ \Gamma_{\bar{2}}^+ &= [1 - R_1^+ R_2^-]^{-1}, & \Gamma_{\bar{2}}^- &= [1 - R_2^- R_1^+]^{-1}. \end{aligned} \quad (15)$$

The adding formulae may be interpreted physically in terms of multiple reflected rays, with the Γ factors being the multiple reflection factors.

The adding method is used in a special way, called the doubling method,^{7,8} to quickly build up the radiative properties of a finite homogeneous layer from the infinitesimal initial layer. The adding algorithm is applied successively to combine two identical layers. Starting with a layer of thickness

$\Delta\tau$, each step doubles the optical depth until after N steps the thickness is $2^N \Delta\tau$. The doubling method described so far requires that the finite layer be uniform. The solar pseudo-source, however, has an exponential dependence with optical depth, and it also is desirable to have the thermal emission vary with depth. The doubling method has been extended by Wiscombe⁹ to incorporate sources that vary exponentially with optical depth and sources that vary linearly with optical depth. For layers that are purely absorbing ($\tilde{\omega} = 0$) the doubling step is bypassed completely by directly computing the properties of the finite layer.

The doubling algorithm computes the reflection and transmission matrices and the source vectors for the homogeneous layers, which are then successively combined, from the top down, with the adding method. The surface boundary is treated as a layer with a transmission of unity, the appropriate reflection, and no source term. The radiation emitted from the surface is then the incident radiation on the lower boundary. The model incorporates two types of surfaces: Lambertian and Fresnel. The radiation downwelling from the atmosphere is computed from the internal radiance algorithm which is easily derived from the interaction principle. Once the radiative properties of the whole atmosphere are found by doubling and adding many boundary conditions, which are Planck radiation from above and the surface properties, can be applied efficiently. The model computes the upwelling radiance from the top of the atmosphere and the downwelling radiance from the bottom of the atmosphere in the form of a Fourier series in azimuth at the discrete quadrature zenith angles.

5. NUMERICAL RESULTS

In order to verify the accuracy of the radiative transfer model and to provide examples for comparison with other models, results from three types of atmospheres are presented. The first case is a Rayleigh atmosphere illuminated by sunlight, the second case is a Mie atmosphere in sunlight, and the third case is microwave transfer through a precipitating atmosphere.

The Rayleigh atmosphere test case was compared with the book of tables by Coulson et al.¹⁰ Comparisons were done for three cases of varying optical depth and solar angle. The radiative transfer model was run with 8 out of the 16 angles in the tables and azimuth modes up to $m = 2$. A quadrature scheme that lets the angles be specified and computes the optimal integration weights was used. The upwelling and downwelling radiances were compared at azimuth angles of 0, 90, and 180° (U is zero at 0 and 180°). Table 1 compares the upwelling radiation for one set of parameters. Note: Coulson et al define Q with a sign opposite to that used here. Table 2 summarizes the Rayleigh case comparison. It shows the average and maximum absolute difference between the Coulson et al tables and the model results for the three cases. Invariably the maximum disagreement is for small μ values. On average the results agree to a few places in the fourth decimal.

6. MIE TEST CASE

The second test case involves a comparison with results from Garcia and Siewert.¹¹ Their $L = 13$ problem used a phase function for Mie scattering at a wavelength of 0.951 μm from a gamma distribution of particles with 0.2 μm effective radius, 0.07 effective variance, and index of refraction

Table 1. Comparison of model output with the results of Coulson et al for a homogeneous Rayleigh atmosphere of optical depth of 1. The upwelling radiance as a function of $\mu = \cos \theta$ for an azimuth of 90° is shown. The solar flux is normalized to π , the cosine of the solar zenith angle is 0.8, and the ground albedo is 0.25.

μ	Present Model			Coulson et al (Ref. 10)		
	I	Q	U	I	Q	U
0.0600	0.39769	-0.05121	0.24707	0.39887	0.05099	0.24758
0.1600	0.40860	-0.03995	0.23359	0.40894	0.03988	0.23375
0.2800	0.40477	-0.02767	0.20914	0.40482	0.02766	0.20918
0.4000	0.39384	-0.01568	0.18112	0.39380	0.01570	0.18114
0.6400	0.37258	0.00779	0.12477	0.37248	-0.00774	0.12476
0.8400	0.36158	0.02686	0.07591	0.36147	-0.02681	0.07590
0.9600	0.35787	0.03813	0.03609	0.35776	-0.03808	0.03609
1.0000	0.35705	0.04168	0.00000	0.35694	-0.04181	0.00000

Table 2. Summary of differences between the radiative transfer model and tables by Coulson et al. The average and maximum absolute differences of the radiances over the eight upwelling zenith angles at azimuths of 0, 90, and 180° are listed for three sets of parameters.

Optical Depth	Solar μ_0	Ground Albedo	Average Error			Maximum Error		
			I	Q	U	I	Q	U
1	0.8	0.25	0.00021	0.00009	0.00007	0.00130	0.00027	0.00051
1	0.2	0.25	0.00021	0.00013	0.00002	0.00160	0.00100	0.00018
0.1	0.1	0.25	0.00041	0.00021	0.00003	0.00175	0.00108	0.00011

$n = 1.44$. Their scattering coefficients ("greek constants"), which are listed in a separate paper,¹² were converted to Legendre series coefficients for the four unique elements of the phase matrix (Table 3).

This test case is for an optical depth of unity and a single scattering albedo of 0.99. The atmosphere is illuminated by a collimated beam at a zenith angle cosine μ_0 of 0.2 with a flux of $\mu_0\pi$ relative to the horizontal. The ground surface is taken to be Lambertian with an albedo of 0.1. Our radiative transfer model produces radiances upwelling from the top of the atmosphere and downwelling from the bottom as Fourier series in azimuth at discrete quadrature zenith angles. Table 4 lists the upwelling radiances for a run with eight Gauss-Legendre quadrature angles per hemisphere and azimuth modes up to $m = 8$. The cosine azimuth modes are listed for I and Q while the sine modes are given for U and V . The initial layer thickness for the doubling algorithm was $\Delta\tau = 10^{-6}$.

Garcia and Siewert's results are tabulated at intervals in μ of 0.1 for azimuths of 0, 90, and 180°. Cubic spline interpolation between the quadrature angles was used to compute the radiances at the tabulated intervals. The values at $\mu = 0$ and 1 were not used as they must be extrapolated from the quadrature angles. The radiative transfer model was run with two different number of quadrature angles (14 and 28) per hemisphere and with azimuth modes up to $m = 9$. A summary of the comparison between the results from the current model and Garcia and Siewert's results are presented in Table 5. Two types of differences were calculated: absolute and fractional. The absolute difference is the absolute value of the difference between the two results. The fractional difference is the absolute difference divided by the maximum value over the zenith angles, separately for each hemisphere and each azimuth angle. The summaries consist of two parts: the average difference and the maximum difference. The summaries include azimuths 0, 90, and 180° for the I and Q terms, but only an azimuth of 90° for the U and V terms.

In general, the maximum fractional differences are from the $\mu = 0.1$ angle which is much less accurate than the other values. Typically, discrete-angle formulations give poorer results for lower μ . The 28-angle case has average fractional differences of about 1 part in 2000, while the differences in the 14 angle case are roughly 5 times worse. Apparently given enough quadrature angles, any desired accuracy can be achieved. The sources of error in this comparison are the approximation inherent in the angular discretization scheme of the model and the interpolation between the quadrature angles. Obviously for most practical uses of the model, a modest number of angles will suffice.

Table 3. Legendre series coefficients for the four unique elements of the phase matrix for the Mie scattering test case.

l	P_1	P_2	P_3	P_4
0	1.00000000	-0.32071711	0.71206342	-0.01882245
1	1.45529318	-0.20350675	1.76014119	-0.04725108
2	1.05402631	0.24638948	1.06682431	0.00894436
3	0.39758994	0.18605748	0.39651104	0.04505815
4	0.11659302	0.07124848	0.09576412	0.00958275
5	0.02387477	0.01700757	0.01765088	0.00215761
6	0.00395010	0.00302534	0.00261549	0.00029195
7	0.00053888	0.00043592	0.00032713	0.00003502
8	0.00006372	0.00005326	0.00003583	0.00000337
9	0.00000667	0.00000572	0.00000351	0.00000029
10	0.00000063	0.00000055	0.00000031	0.00000002
11	0.00000006	0.00000005	0.00000003	0.00000000

Table 4. Results from the Mie scattering test case. Upwelling radiances (I, Q, U, V) are expressed as a Fourier series in azimuth for the eight Gauss-Legendre quadrature zenith angles. The cosine modes for I and Q and the sine modes for U and V are listed. See the text for details of modeling parameters.

μ	$m=0$	$m=1$	$m=2$	$m=3$	$m=4$	$m=5$	$m=6$	$m=7$	$m=8$
Upwelling I									
0.09501	3.16625(-1)	2.99208(-1)	1.41050(-1)	3.91377(-2)	9.49855(-3)	1.68971(-3)	2.49391(-4)	3.07795(-5)	3.32533(-6)
0.28160	2.13111(-1)	1.68949(-1)	7.68883(-2)	1.98090(-2)	4.64431(-3)	7.96683(-4)	1.13692(-4)	1.35392(-5)	1.41070(-6)
0.45802	1.52211(-1)	1.02308(-1)	4.46789(-2)	1.04513(-2)	2.29646(-3)	3.66285(-4)	4.86577(-5)	5.37863(-6)	5.19893(-7)
0.61788	1.13203(-1)	6.29048(-2)	2.56453(-2)	5.24027(-3)	1.03555(-3)	1.46891(-4)	1.73606(-5)	1.70182(-6)	1.45805(-7)
0.75540	8.76554(-2)	3.83168(-2)	1.38881(-2)	2.34463(-3)	3.93630(-4)	4.68113(-5)	4.63932(-6)	2.72140(-8)	3.80182(-7)
0.86563	7.11167(-2)	2.25849(-2)	6.68693(-3)	8.57039(-4)	1.11977(-4)	1.02395(-5)	7.79929(-7)	4.90429(-8)	2.68677(-9)
0.94458	6.10150(-2)	1.21975(-2)	2.50940(-3)	2.09890(-4)	1.82694(-5)	1.10023(-6)	5.52094(-8)	2.32459(-9)	8.21768(-11)
0.98940	5.58402(-2)	4.81263(-3)	4.54656(-4)	1.67729(-5)	6.51588(-7)	1.74252(-8)	3.89063(-10)	2.54257(-11)	1.13266(-13)
Upwelling Q									
0.09501	6.35745(-2)	1.95402(-2)	-4.85223(-2)	-2.07407(-2)	-6.20378(-3)	-1.26607(-3)	-1.99414(-4)	-2.58918(-5)	-2.88223(-6)
0.28160	4.06995(-2)	-6.96796(-4)	-3.64520(-2)	-1.33381(-2)	-3.71525(-3)	-7.21511(-4)	-1.08842(-4)	-1.35642(-5)	-1.45020(-6)
0.45802	2.52572(-2)	-7.97154(-3)	-3.09958(-2)	-9.33185(-3)	-2.52362(-3)	-4.51094(-4)	-6.28151(-5)	-7.23389(-6)	-7.14809(-7)
0.61788	1.49899(-2)	-1.09466(-2)	-2.77641(-2)	-7.66889(-3)	-1.72014(-3)	-2.71741(-4)	-3.34518(-5)	-3.40558(-6)	-2.97378(-7)
0.75540	8.27355(-3)	-1.10523(-2)	-2.54804(-2)	-5.80368(-3)	-1.44314(-4)	-1.48319(-5)	-1.48319(-5)	-1.25964(-6)	-0.16897(-8)
0.86563	4.02847(-3)	-9.28289(-3)	-2.37064(-2)	-4.12199(-3)	-5.99753(-4)	-6.08586(-5)	-4.79347(-6)	-3.11648(-7)	-1.73499(-8)
0.94458	1.52144(-3)	-6.37584(-3)	-2.24488(-2)	-2.56325(-3)	-2.47374(-4)	-1.65465(-5)	-8.57109(-7)	-3.66272(-8)	-1.33780(-9)
0.98940	2.76513(-4)	-2.87733(-3)	-2.17265(-2)	-1.09920(-3)	-4.72883(-5)	1.40403(-6)	-3.22879(-8)	-6.21991(-10)	-9.86357(-12)
Upwelling U									
0.09501		4.65680(-2)	2.96372(-2)	9.39333(-3)	2.24573(-3)	4.05235(-4)	5.90103(-5)	7.25006(-6)	7.76362(-7)
0.28160		3.64936(-2)	2.97577(-2)	9.73701(-3)	2.45917(-3)	4.53193(-4)	6.61923(-5)	8.07079(-6)	8.50006(-7)
0.45802		2.83557(-2)	2.87641(-2)	8.80381(-3)	2.13216(-3)	3.71494(-4)	5.09304(-5)	5.80459(-6)	5.69497(-7)
0.61788		2.16460(-2)	2.71199(-2)	7.35609(-3)	1.61396(-3)	2.52014(-4)	3.08059(-5)	3.12159(-6)	2.71714(-7)
0.75540		1.59988(-2)	2.53115(-2)	5.73356(-3)	1.07001(-3)	1.40703(-4)	1.44216(-5)	1.22254(-6)	8.88861(-8)
0.86563		1.13368(-2)	2.36822(-2)	4.11089(-3)	5.96606(-4)	6.04597(-5)	4.75821(-6)	3.09132(-7)	1.72077(-8)
0.94458		6.83317(-3)	2.24467(-2)	2.56234(-3)	2.47179(-4)	1.65299(-5)	8.56015(-7)	3.65348(-8)	1.33609(-9)
0.98940		2.91467(-3)	2.17265(-2)	1.09918(-3)	4.72871(-5)	1.40399(-6)	3.21707(-8)	6.01155(-10)	9.86313(-12)
Upwelling V									
0.09501		-6.77792(-5)	4.81852(-5)	3.23701(-5)	1.08929(-6)	3.26912(-8)	5.06132(-10)	6.13565(-12)	5.29244(-14)
0.28160		-2.27332(-5)	-8.79580(-5)	-6.56752(-6)	-3.05365(-7)	-7.81300(-9)	-1.21795(-10)	-1.36489(-12)	-1.13640(-14)
0.45802		2.13234(-5)	-1.14599(-4)	-1.21151(-5)	-4.26800(-7)	-1.03864(-8)	-1.45053(-10)	-1.50495(-12)	-1.14565(-14)
0.61788		4.99363(-5)	1.00813(-4)	-9.37357(-6)	-2.89817(-7)	-6.21234(-9)	-7.61919(-11)	-6.96535(-13)	-4.67381(-15)
0.75540		6.18229(-5)	-7.27901(-5)	-5.63970(-6)	-1.41115(-7)	-2.50873(-9)	-2.55689(-11)	-1.94210(-13)	-1.08500(-15)
0.86563		5.86359(-5)	-4.29711(-5)	-2.48601(-6)	-4.74308(-8)	-6.41946(-10)	-4.99276(-12)	-2.88649(-14)	-1.23406(-16)
0.94458		4.34734(-5)	-1.84950(-5)	-6.89434(-7)	-8.62443(-9)	-7.63524(-11)	-3.88909(-13)	-1.42709(-15)	-4.12509(-18)
0.98940		2.04401(-5)	-3.61377(-6)	-5.88912(-8)	-3.26520(-10)	-1.27732(-12)	-2.81285(-15)	1.73723(-17)	-5.92740(-21)

Table 5. Summary of differences between the radiative transfer model and results from Garcia and Siewert for their $L = 13$ Mie scattering problem. The model is compared for two runs having 14 and 28 quadrature angles per hemisphere respectively. The summary incorporates results from radiances upwelling from the top and downwelling from the bottom of the atmosphere for nine zenith angles and three azimuth angles.

Summary of 14 angle case				
Absolute differences				
	I	Q	U	V
Average	0.00048	0.000111	0.0000278	0.00000032
Maximum	0.00621	0.001190	0.0001210	0.00000134
Fractional differences				
	I	Q	U	V
Average	0.0020	0.0032	0.0010	0.0037
Maximum	0.0078	0.0362	0.0031	0.0090
Summary of 28 angle case				
Absolute differences				
	I	Q	U	V
Average	0.00010	0.000021	0.0000083	0.00000009
Maximum	0.00141	0.000176	0.0000402	0.00000050
Fractional differences				
	I	Q	U	V
Average	0.0004	0.0005	0.0003	0.0009
Maximum	0.0013	0.0024	0.0009	0.0032

7. MICROWAVE EXAMPLE

The third case is different from the first two in having thermal sources of radiation rather than a collimated solar source. The radiance field in a plane-parallel atmosphere with only thermal radiation is azimuthally symmetric and has zero U and V components. While this case does not include a validation, the thermal source aspects of the model have been tested against the unpolarized model of Stamnes et al¹³ with agreement to better than 1 part in 10^5 . For simplicity, we now consider a two layer precipitating atmosphere having an ice layer above a rain layer. Both layers have Marshall-Palmer¹⁴ (exponential) particle size distributions with a maximum diameter of 1.0 cm. The modeled precipitation is quite light: the rain layer has a rain-rate of 0.5 mm/h and the ice layer has a M-P rain rate of 2.0 mm/h. The single scattering properties of the water and ice spheres are computed according to Mie theory. Absorption by oxygen, water vapor, and cloud liquid water is ignored. Table 6 lists the properties of the atmosphere and Table 7 contains the Legendre series coefficients for the phase matrices. The modeling frequency is 85.5 GHz which is the highest microwave frequency currently in use on an orbiting platform (the Special Sensor Microwave/Imager instrument). The surface is modeled as calm water by a Fresnel surface with the appropriate index of refraction ($3.724 - 2.212i$) for water at 27°C. Cosmic black body radiation at 2.7 K is incident from above.

For this case, we assume the Rayleigh-Jeans approximation for the Planck function and output brightness temperatures rather than radiances. The model is run with eight Gaussian quadrature angles, one Fourier azimuth mode ($m = 0$), and two Stokes parameters (I and Q). Table 8 gives the results for the brightness temperatures upwelling from the top and the downwelling from the

Table 6. Properties of the two layer atmosphere for 85.5 GHz microwave case. The heights and temperatures refer to the layer interfaces. The rain rate specifies the Marshall-Palmer distribution of hydrometeors with the given indices of refraction. The extinction and single scattering albedo from the Mie calculation is also listed.

Layer	Height (km)	Top Temp (Kelvin)	Rain Rate (mm/hr)	Index of refraction	Extinction (km^{-1})	Albedo
Ice	8.0	245	2.0	(1.7829, -.00344)	0.13536	0.98190
Rain	4.0	273	0.5	(3.2781, -1.8512)	0.15224	0.38175
	0.0	300				

Table 7. Legendre series coefficients for the three required elements of the phase matrices for the microwave test case. The coefficients are listed for the rain and ice layers. Only P_1 , P_2 , and P_3 are needed when using just two Stokes parameters (I and Q).

l	Rain Layer			Ice Layer		
	P_1	P_2	P_3	P_1	P_2	P_3
0	1.000000	-0.378560	0.122149	1.000000	-0.203665	0.706712
1	0.365211	-0.082115	1.482953	1.305650	-0.111353	1.669173
2	0.518055	0.353963	0.356369	0.915656	0.176185	0.856457
3	0.115569	0.077666	0.067922	0.348084	0.097906	0.357357
4	0.032699	0.023756	0.008445	0.131959	0.025961	0.114952
5	0.006058	0.004312	0.001049	0.032286	0.012476	0.031836
6	0.001139	0.000819	0.000071	0.011950	0.001494	0.009323
7	0.000188	0.000133	0.000000	0.001923	0.000916	0.002046
8	0.000030	0.000021	-0.000002	0.000899	0.000030	0.000561
9	0.000005	0.000003	0.000000	0.000085	0.000052	0.000112
10				0.000061	-0.000004	0.000025
11				0.000003	0.000003	0.000006
12				0.000004	-0.000001	0.000001

bottom of the precipitating atmosphere. For comparison the brightness temperatures upwelling from the surface without any atmosphere are also given. Although the atmospheric model is over-simplified, the results clearly show the sensitivity of 85 GHz to low rain-rates over a water surface. The absorption and emission of the rain layer increases the upwelling brightness temperature, while the scattering of the ice layer acts to decrease the brightness temperature. Both layers depolarize the radiation because the precipitation particles are modeled by spheres.

8. CONCLUDING REMARKS

We have described a polarized plane-parallel radiative transfer model for randomly-oriented particles of arbitrary shape. The model is designed for passive atmospheric remote sensing applications, whether reflection or emission based. The formulation described in this paper is perhaps the simplest of the many solution methods to the polarized radiative transfer problem. The simplicity is evident both in the direct method of transforming the single scattering information and the use of the doubling and adding method. While not as accurate as some other methods, doubling and adding is robust and provides adequate accuracy for practical problems within reasonable running times. The results from several example computations are shown, which verify the accuracy of the model and provide results for comparison. An efficiently coded and well documented FORTRAN implementation of the model is available for distribution. More complete information about the model is available in a report.¹⁵ A closely related code that models polarized radiative transfer through oriented non-spherical particles has been used to compute microwave transfer through horizontally-oriented ice crystals.¹⁶

Table 8. Brightness temperature results for the microwave test case. The upwelling radiances from the top of the atmosphere and the downwelling radiances from the bottom of the atmosphere and tabulated in Kelvin. For comparison, the upwelling brightness temperatures from the surface without an atmosphere are also listed.

μ	Upwelling		Downwelling		No atmosphere	
	I	Q	I	Q	I	Q
0.09501	111.89	0.68	270.09	5.58	127.13	102.88
0.28160	154.71	2.81	244.50	4.34	169.19	107.04
0.45802	184.41	4.66	210.27	3.03	169.81	76.63
0.61788	200.67	5.44	181.84	1.95	167.63	49.82
0.75540	208.90	4.71	161.00	1.14	166.27	29.64
0.86563	212.88	3.08	146.60	0.58	165.68	15.37
0.94458	214.70	1.41	137.42	0.23	165.50	6.09
0.98940	215.43	0.28	132.58	0.04	165.46	1.14

Acknowledgement—This work was supported by the National Aeronautics and Space Administration under Grant NAG8-643.

REFERENCES

1. S. Chandrasekhar, *Radiative Transfer*, Dover, New York, NY (1960).
2. J. W. Hovenier, *J. Atmos. Sci.* **26**, 488 (1969).
3. J. V. Dave, *Appl. Optics* **9**, 2673 (1970).
4. A. Ishimaru, D. Lesselier, and C. Yeh, *Radio Sci.* **19**, 1356 (1984).
5. J. E. Hansen, *J. Atmos. Sci.* **28**, 120 (1971).
6. W. J. Wiscombe, *J. Atmos. Sci.* **34**, 1408 (1977).
7. H. C. van de Hulst, "A New Look at Multiple Scattering," Goddard Institute for Space Studies, NASA, New York, NY (1963).
8. I. P. Grant and G. E. Hunt, *Proc. R. Soc. Lond.* **A313**, 183 (1969).
9. W. J. Wiscombe, *JQSRT* **16**, 637 (1976).
10. K. L. Coulson, J. V. Dave, and Z. Sekera, *Tables Related to Radiation Emerging from a Planetary Atmosphere with Rayleigh Scattering*, Univ. of California Press, Berkeley, CA (1960).
11. R. D. M. Garcia and C. E. Siewert, *JQSRT* **41**, 117 (1989).
12. P. Vestrucci and C. E. Siewert, *JQSRT* **31**, 177 (1984).
13. K. Stamnes, S.-C. Tsay, W. Wiscombe, and K. Jayaweera, *Appl. Optics* **27**, 2502 (1988).
14. L. J. Battan, *Radar Meteorology*, Univ. of Chicago Press, Chicago, IL (1959).
15. K. F. Evans and G. L. Stevens, "Polarized Radiative Transfer Modeling: an Application to Microwave Remote Sensing of Precipitation," Colorado State University, Department of Atmospheric Science Paper No. 461, Fort Collins, CO (1990).
16. K. F. Evans and J. Vivekanandan, *IEEE Trans. Geosci. Remote Sensing* **28**, 423 (1990).